Review

Recent Progress on Highly Selective and Sensitive Electrochemical Aptamer-based Sensors

TANG Tianwei[1#], LIU Yinghuan[1#] and JIANG Ying[1,2]✉

Received March 10, 2022
Accepted April 10, 2022

Highly selective, sensitive, and stable biosensors are essential for the molecular level understanding of many physiological activities and diseases. Electrochemical aptamer-based (E-AB) sensor is an appealing platform for measurement in biological system, attributing to the combined advantages of high selectivity of the aptamer and high sensitivity of electrochemical analysis. This review summarizes the latest development of E-AB sensors, focuses on the modification strategies used in the fabrication of sensors and the sensing strategies for analytes of different sizes in biological system, and then looks forward to the challenges and prospects of the future development of electrochemical aptamer-based sensors.

Keywords Electrochemical biosensor; Aptamer; Biomolecular recognition; Biological system

1 Introduction

Biosensors have been widely used in qualitative and quantitative analysis in complexed biological systems[1]. They play vital roles in the fields of clinical medicine[2], pathology[3], human immunology[4], pharmacy[5], environmental science[6] and other fields. Particularly, the pandemic situation has further advanced the biosensors to meet the requirements of practical applications, and thus more efficient, sensitive, stable and portable biosensors have brought into the sharp focus of the field[7−10]. Usually, biosensors mainly rely on electricity[11], heat[12] and optics[13] to transform the concentration and distribution of analytes, including neurotransmitters, metabolites, enzymes, antigens, antibodies, viruses, and cells in biological systems into detectable signal responses[14−19]. While a variety of affinity ligands, including aptamers, antibodies, and enzymes can be used as the recognition elements of the sensors[20−23], aptamer-based sensors, particularly electrochemical aptamer-based sensors have become the focus of sensor field, attributed from their high selectivity and sensitivity, flexibility and diverse design[24−33].

Aptamers, including RNA aptamers and DNA aptamers are a class of single stranded oligonucleotide molecules with a specific recognition function[34−36]. They are nucleotide sequences with recognition ability for specific substances selected from a series of nucleotide sequences by systematic evolution of ligands by exponential enrichment(SELEX)[37−40]. Aptamers have the characteristics of high selectivity and excellent biological affinity. Compared with other specific recognition molecules, such as enzymes and antibodies, aptamers have the advantages of flexible structure and chemical composition, diverse modification and sensing strategies, and can be adapted to a variety of detection systems[41−48]. Moreover, aptamers have been continually combined with emerging materials, such as carbon nanomaterials[49−51] and metal nanoparticles[52−54], and have found remarkable applications in a variety of fields, including cell cancer diagnosis[55−57], targeted drug innovation[58−60], judicial detection[61−63] and many others.

When aptamers bind to target molecules, the intermolecular interaction alters the configuration or chemical environment of the aptamer, which may change the electrochemical properties, such as electron transfer rate and interface properties[64−66]. Based on this, scientists have created a great panel of electrochemical biosensors that rely on aptamers for highly selective recognition[67−69]. Electrochemical aptamer-based(E-AB) sensors not only merit the advantages of aptamers, but also have the advantages of fast analysis rate and high sensitivity of electrochemical analysis methods. Up to now, some E-AB sensors can reach sensitivity down to fmol/L level[70−72]. Together with their excellent anti-interference ability, adaptability with portable devices, E-AB sensors hold great promise for practical application[73]. In this minireview, we summarize the latest development of E-AB sensors, and focus on the modification strategies used in the fabrication of sensors and the sensing strategies for analytes of different sizes in biological system.

2 Fabrication of E-ABs

To build a selective and sensitive E-AB sensor, one of the most critical steps is to stably modify aptamers on the electrode surface[74]. Because the nucleic acid has many reactive sites, the

✉ JIANG Ying
yingjiang@bnu.edu.cn
# These authors contributed equally to this work.
1. College of Chemistry, Beijing Normal University, Beijing 100875, P. R. China;
2. Beijing National Laboratory for Molecular Sciences, Beijing 100190, P. R. China

https://doi.org/10.1007/s40242-022-2084-z

structure of aptamer can be easily designed to modify the reactive groups, so that the aptamer can form a stable structure through covalent or non-covalent interaction with the electrode surface[75−77].

2.1 Covalent Strategy

Covalent strategies refer to the formation of covalent bonds between aptamers and electrode surface. They are the most commonly used modification strategies in the process of aptamer modification. Most E-AB sensors are fabricated by covalent strategies[78−85]. With the advantages of stable bonding and simple steps, covalent strategies can directly combine aptamers with the electrode surface stably[86,87].

One of the most common covalent strategies is to modify aptamers on the surface of gold electrodes or on gold nanoparticles attached to the electrode surface by gold-sulfur bonds(Au—S)[88−93]. This kind of modification strategy is simple, can be carried out at room temperature, and the modification process is not limited by the shape of the electrode. It can be applied to gold micro electrodes and gold nanoparticles to meet the requirements of portable sensors. Xiao *et al*.[94] reported a portable paper E-AB sensor that can be applied to *in-situ* detection. After modifying a single-layer carbon nanotube film on the paper in vacuum atmosphere, gold nanoparticles are deposited on it to form a "three electrodes" system, and then the aptamer with a sulfhydryl group at the 5' end and methylene blue(MB) at the 3' end is modified on the electrode. After passivation with blocking agent on the electrode surface, the as-generated sensor can be used for the measurement of cocaine and methylenedioxypyrovalerone(MDPV) in both serum and saliva[Fig.1(A)]. The detection limits of cocaine and MDPV of the sensor in the calf serum are 5 and 1 μmol/L, respectively, demonstrating the sensitivity of E-AB sensors in the complex environment.

Connecting aptamers with gold nanoparticles through Au—S bond gives this covalent strategy flexibility, which can make it obtain greater advantages by combining gold nanoparticles with other materials[95−99]. Xu *et al*.[100] reported a modification strategy of modifying the carbon electrode by combining multi-layer carbon nanotubes with gold nanoparticles, and then connecting with the aptamers through Au—S bond. This modification method increased the effective modification area and the conductivity of the electrode surface, resulting in the higher signal response and more aptamers for higher selectivity. The detection limit of long non-coding RNAs(lncRNAs) by differential pulse voltammetry(DPV) method is down to 42.8 fmol/L, and the linear range is 0.01 pmol/L—10 nmol/L. Compared with the interfering substance at 50 pmol/L, the target substance at 1 pmol/L can produce a significant signal response.

Stability, flexibility, cost and adaptability of electrodes are several factors that must be considered in the selection of modification strategy in the fabrication process. With the development of electrochemistry, carbon electrodes show excellent performance and gradually become one of the main electrodes. In this system, the application of Au—S bond is greatly limited. For carbon electrode system, it is a common modification strategy to generating stable amide bonds (—CO—NH—) by using 1-(3-dimethylaminopropyl)-3-ethylcarbodiimide hydrochloride(EDC) and *N*-hydroxy succinimide(NHS) activated carboxyl groups and amino modified aptamers[78−80]. Amide bond has the advantages of strong stability, diverse generation strategies, flexible design and wide application system[101−103]. It can be applied to the modification of carbon electrodes, emerging carbon materials and metal nanoparticles[104−106]. New materials, such as graphene and metal nanoparticles have the advantages of good conductivity, stable adhesion, strong chemical reactivity and large surface area. When they are combined with aptamers, improved amounts of aptamers are modified on electrodes, offering higher selectivity and sensitivity of sensors[107−109].

Liang *et al*.[79] reported a sensor combining aptamer with graphene oxide(GO) on the surface of glassy carbon electrode, which can be used for detecting α-fetoprotein(AFP). Firstly, the oxygen-containing groups on the surface of GO were oxidized to carboxyl group through the mixed solution of chloroacetic acid and sodium hydroxide, and then they could bond with the aptamers modified with amino group through amide bond. The 20-folds interfering proteins PSA and CEA have not caused obvious signal response, demonstrating its high selectivity. The detection limit is 3 pg/mL[Fig.1(B)]. In another example, Upan *et al*.[80] reported a sensor, in which PtNP/GO-COOH nanoparticles were generated from GO and platinum by the aqueous phase reduction method, modified on the surface of glassy carbon electrode and formed amide bond with the AFP aptamers. This sensor showed high selectivity and sensitivity with a detection limit achieving 1.22 ng/mL by square wave voltammetry(SWV) method.

When covalent strategies carried out on the electrode surface, it is difficult to ensure that aptamers completely cover the whole electrode surface. In order to prevent electrochemical active substances from reacting on the unmodified electrode surface and producing false-positive electrical signals, it is usually necessary to add blocking agents to passivate the unmodified area on the electrode surface[110]. There are three types of passivation strategies, a) blocking the unmodified region after the modification of aptamers; b) pre-blocking the electrode surface, then aptamers covalently linked with the terminal group of the blocking agent; c) the blocking agent and aptamers added to the system

https://doi.org/10.1007/s40242-022-2084-z

simultaneously, competing for binding on the electrode surface[Fig.1(C)].

Mercaptohexanol(MCH) is a blocking agent often used in gold electrode system because of its strong Au—S binding ability and mild reaction conditions[111−115]. Moreover, MCH is difficult to be protonated or deprotonated in the detection system, thus reduces the impact of electrostatic interaction and provides a better passivation effect[116]. Recently, increasing studies have shown that the ratio of aptamer to MCH also significantly affects the performance of sensors. When fabricating the sensor of tenofovir(TFV), Aliakbrinodehi *et al*.[117] found that the sensor showed the highest signal response when the ratio of aptamer to MCH was 1:100 [Fig.1(D)]. Higher or lower ratio will lead to the decrease of response value. This is probably because at a lower ratio, aptamers cannot fully capture the targets, while at a higher ratio, not all aptamers on the electrode surface change their configuration completely when capturing the targets due to the influence of steric resistance and electrostatic repulsion, which hinders the rate of electron transfer. Other than MCH, bovine serum albumin(BSA) is also a widely used blocking agent[118−122]. BSA has a large number of amino and carboxyl groups on the surface, so it can combine with both hydrophilic and hydrophobic surfaces to inhibit the nonspecific binding on the electrode surface[123].

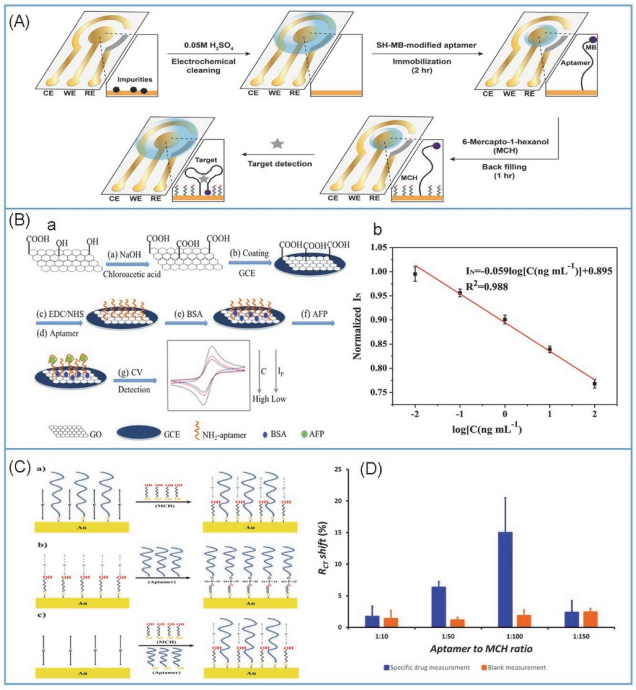

Fig.1 Sensors fabricated by covalent strategies

(A) Schematic illustration of aptamer-based paper electrochemical device(PED) fabrication process and detection process. Reprinted with permission from Ref.[94], Copyright 2021, Wiley-VCH; (B) schematic illustration of fabrication process of GO-based E-AB sensor for AFP detection(a), and the calibration curve of GO-based E-AB sensor for AFP detection(b). Reprinted with permission from Ref.[79], Copyright 2018, Elsevier; (C) schematic illustration of three kinds of passivation strategies; (D) different RCT shift responses at different ratios of aptamer to MCH[blue bars indicate the electrochemical impedance spectroscopy (EIS) response of sensors to 500 nmol/L TFV at different aptamer-to-MCH ratios]. Reprinted with permission from Ref.[117], Copyright 2017, Springer Nature.

2.2 Noncovalent Strategy

Noncovalent strategies refer to the connection of aptamers and electrode surface through electrostatic adsorption, hydrogen bonding, van der Waals interactions, etc. Compared with covalent strategies, noncovalent strategies exhibit unique advantages, such as less strict requirements for aptamer modification, wider application field, and more flexible design[124]. They are relatively straightforward and can quickly realize the assembly and functionalization of sensors.

Streptavidin is a protein composed of four peptide chains. It can form a very strong interaction with biotin through noncovalent interaction. The extremely low dissociation constant(K_d=10^{-15} mol/L) demonstrates that this interaction is very stable[125]. By modifying streptavidin on the electrode surface and biotin on the 5' end of the aptamers, the aptamers can be efficiently modified on the electrode surface. On this basis, the strategy can be further developed by combining with nano materials to obtain better signal response. Gopinath *et al*.[126] reported a sensor using streptavidin and biotin to modify the complex of aptamers and gold nanoparticles on the electrode, and verified that the signal response of the sensor employing gold nanoparticles was higher than that of the platform without gold nanoparticles. Compared with the platform without gold nanoparticles, the detection limit decreased to 10 times lower.

The application of various materials also provides more possibilities for the improvement of the selectivity and sensitivity of sensors. Cai *et al*.[127] reported a method of combining GO, thionine, chitosan and streptavidin modified gold nanoparticles to form a modified electrode, and then combined with biotin modified aptamers to form a sensor. This strategy enhanced the loading efficiency of the aptamers, leading to a great sensitivity with a detection limit of 10 pg/mL for estrogen(17β-e2).

Though noncovalent strategies have a wide range of applications, they are prone to be affected by different types and structures of aptamers. Zhang *et al*.[128] reported that few or single-layer nano disulfide transition metal layers, such as MoS_2, TiS_2 and TaS_2, could strongly interact with single stranded DNA(ssDNA), but no longer have such interaction with double stranded DNA(dsDNA). The reason is that the strong interaction stems from the interaction between the nano layer and the nitrogenous bases in nucleotides. Therefore, in double stranded DNA, the bases are shielded, resulting in the reduction of the interaction. The distinct binding between ssDNA and dsDNA to the functional material surface provides the possibility for designing special sensing strategies. For example, Wang *et al*.[129] reported a new sensor using a MoS_2

https://doi.org/10.1007/s40242-022-2084-z

modified glassy carbon electrode. Y-Type detection molecules composed of lead chain, assist chain and aptamer cannot bind to the electrode surface without target. In the presence of targets, the aptamer is removed to leave a single chain structure, which can interact with the electrode surface and generate a response signal. The detection limit for kanamycin of the sensor is 29 pmol/L[Fig.2(A)]. Benefited from this modification strategy, the selectivity of the sensor was further increased, and the other 17 antibiotic interfering substances did not have a noticeable effect on the signal.

As the direction of biosensor miniaturization, fiber electrode provides an appealing candidate for biological *in vivo* measurement. In this case, carbon fiber electrode(CFE) is favored because of its high stiffness, good conductivity and minimal biological damage. Recently, we reported a microsensor fabricated by noncovalent modification of aptamers on the surface of carbon fiber electrode[130]. Specifically, we pre-modified the CFE surface with *n*-hexamine chain by electrooxidation method, and then the aptamers with cholesterol-modification at its 5' end can spontaneously assemble on the alkyl chain layer through hydrophobic interaction to form an aptCFE sensor. We implanted this micro sensor into the brain of mice. After current stimulation, the sensor successfully captured the signal of rapid release of dopamine in the nervous system, demonstrating the excellent features of this micro sensor for *in vivo* measurement[Fig.2(B)]. The fabrication of the sensor is simple and efficient, and can be generalized, and thus ideally this platform can be employed for *in vivo* detection of many other neurotransmitters, providing effective tools for studying the nervous system.

In conclusion, the aptamer modification strategies in various E-AB sensors are diverse and have their own advantages and limitations(Table 1 and Fig.3). The modification strategies need to be selected according to the sensing strategy, application environment and cost requirements of the sensor to ensure that the interaction between aptamers and the electrode is stable and feasible. With new surface chemistries emerging, more approaches can be expected for creating efficient and stable E-AB sensors.

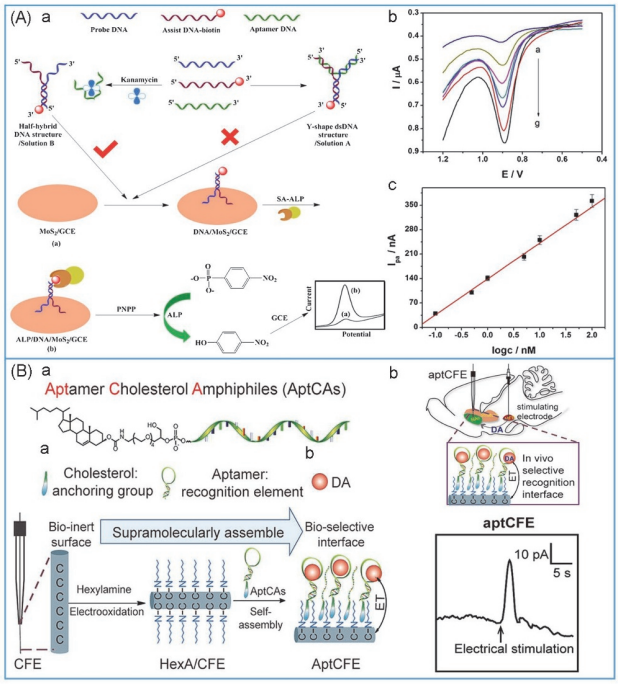

Fig.2 Sensors fabricated by noncovalent strategies

(A) Schematic illustration of the detection process of the sensors based on the Y-shape DNA absorbed on the MoS_2 nanosheet and amplification effect by using ALP catalyzed process(a), different DPV response to different concentration of kanamycin(b), and the linear relationship between the logarithm value of kanamycin concentration and DPV peak current(c). Reprinted with permission from Ref.[129], Copyright 2019, Elsevier; (B) schematic illustration of the cholesterol-modified aptamer and their self assembly process on CFE for a bio-selective electro-chemical interface(a), and schematic illustration of aptCFE for *in vivo* DA sensing and the current responses of aptCFE in the rat NAc upon electrical stimulation of rat MFB(b). Reprinted with permission from Ref.[130], Copyright 2020, Wiley-VCH.

Table 1 Comparison of common modification strategies

Modification type	Modification strategy	Aptamer modification	Advantage	Limitation	Ref.
Covalent	Au—S(gold-sulfur bond)	Thiol group	1. Stable binding 2. Simple modification 3. Suitable for Au electrode and not limited by the shape	1. Increased cost 2. Not suitable for nongold system	[88—99,131]
	—CO—NH— (amide bond)	Amine group	1. Strong stability 2. Low cost 3. Diverse generation reagents and strategies 4. Flexible design and wide applications	1. Need to activate carboxyl groups 2. May need crosslinkers	[101—109,131]
Noncovalent	Streptavidin-biotin	Biotin group	1. Strong interaction 2. Simple modification	1. High cost 2. Complex steps	[125—127,131]
	Nano XS_2 layers-nitrogenous base, X=Mo, Ti, Ta	Single strand DNA	1. Selective attraction of single stranded DNA 2. Singal intensity is not limited by the amount of modified aptamer 3. Effective in specially designed sensors	1. Complex preparation for nano material 2. Special design for sensing strategy 3. Requirement for detection system	[128,129]
	Alkyl layers-cholesterol	Cholesterol group	1. Low cost 2. Simple modification 3. It can be applied in micro electrode and *in vivo* detection	1. Sensitive to temperature 2. Need special modified aptamer 3. Relatively weak interaction	[130]

https://doi.org/10.1007/s40242-022-2084-z

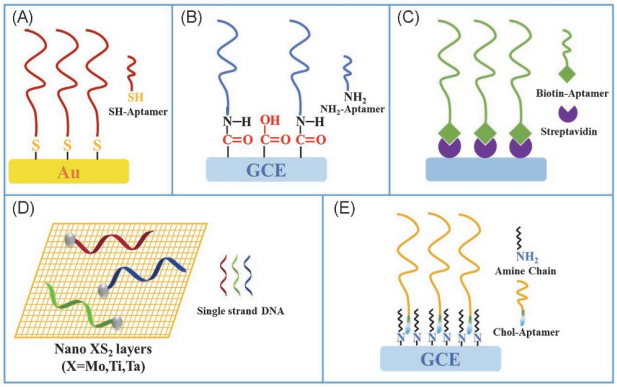

Fig.3 Schematic illustration of modification strategies

(A) Covalent strategy: Au—S bond; (B) covalent strategy: amide bond; (C) noncovalent strategy: streptavidin-biotin interaction; (D) noncovalent strategy: nano XS_2 layers-nitrogenous base interaction, X=Mo, Ti, Ta; (E) noncovalent strategy: alkyl layers-cholesterol interaction.

3 Applications of E-ABs

The application scope of the biosensor mainly depends on its sensitivity, selectivity, and stability, which requires the detection limit of the sensor to be lower than the actual concentration of the detection environment, quick response, and not to be disturbed or affected by interfering substances[31,132,133]. Up to date, E-ABs have been applied for the sensing of a variety of analytes, including small molecules, macromolecules and large analytes such as cells and viruses.

3.1 Sensing of Small Molecules

Small biological molecules, such as neurotransmitters, metabolites and cell secretions play a vital regulatory role in the biological system[134−136]. The detection of biological small molecules is of great significance for understanding the mechanism of biological activities and disease monitoring. Due to the high selectivity and sensitivity of aptamers, E-AB sensors have been widely used in the actual detection of a variety of biological small molecules[137−139]. Based on the electrochemical properties of these small molecules, they can be divided into electroactive or electroinactive analytes.

3.1.1 Electroactive Analytes

For the sensing of electroactive analytes, the flexible aptamer chain captures the target, wraps around the small molecule, and makes the small molecule close to the electrode surface for electron transfer. In fact, few electroactive substances, such as dopamine are suitable for sensing in this direct way[140−142]. However, in many cases, when the aptamer wraps the targeted molecule, it shields the signal of the analyte. In addition, this direct sensing strategy has no amplification effect. Thus, the signal response is limited to the amount of modified aptamers and the concentration of the analyte, and the signal response is usually not as good as indirect sensing[143−145]. The detection limit of the sensor sensing in a direct way by the oxidation of dopamine is usually nmol/L level, which could be further improved with the assistance of nano materials with high conductivity[146,147].

Because the electrochemical signal is generated from the analyte itself in the direct sensing based approach, the fabrication steps of the sensors for electrochemical active substance are relatively simple and can be applied to a variety of systems, especially biological systems. For example, Ferapontova *et al*.[148] reported a sensor that could be directly applied to undiluted human serum to detect the concentration of dopamine. The dopamine RNA aptamers and cysteine are modified on the surface of the electrode. Cysteine is included to serve as both a blocking agent as well as positively charged molecules for electrochemical interaction with aptamers, so that the aptamers can spread on the surface of the electrode and capture the target. Using an amperometry method, the detection limit of the sensor for dopamine in undiluted human serum is 114 nmol/L and the linear range is 0.1—2 μmol/L.

3.1.2 Electroinactive Analytes

In biological systems, many small molecules, such as gas molecules and metabolic substances do not have electrochemical activity or require a high potential to generate electrical signals, so they need the assistance of other signal substances to generate signals through the changes of electrode interface chemical environment[149−153]. Indirect sensing strategies of electroinactive analytes have the advantage that the signal intensity does not directly depend on the number of aptamers modified on the electrode, so the detection limit can be further improved, and can be applied to complex environments with higher selectivity. However, compared with direct sensing, the fabrication of the sensor is usually more complex, the cost may be higher, and more factors need to be considered in design.

Since the target substance itself does not have electrochemical activity, one of the most common strategies is to modify the electrochemically active groups on the aptamer, such as methylene blue(MB), which is usually modified at one end of the aptamer. When the aptamer does not bind to the target substance, the nucleic acid chain stretches, the electrochemical active group is far away from the electrode surface, and the electron transfer rate is slow. When the configuration of the aptamer binding target changes, the electrochemically active group is close to the electrode surface, the electron transfer rate is accelerated, and a larger current response signal is generated, which is positively correlated

https://doi.org/10.1007/s40242-022-2084-z

with the concentration of the target substance[154−158]. White *et al*.[82] reported a sensor that modified the gold electrode with MB-modified aptamers. When the aptamer captured the target, MB approached to the electrode and electron transfer occurred, and electrons of indicator electrode prussian white(PW) were lost on the color plate connected with the sensing electrode to make PW become prussian blue(PB)[Fig.4(A)]. Based on the process, the colorimetric method can be used to detect the concentration of ATP.

In addition to modifying electrochemical active groups, the method of inserting electrochemical indicators is also very common. The most commonly used one is ruthenium complex ions that can bind to the nucleic acid chain skeleton through non-covalent interactions and generate electrochemical signals. Since a single aptamer can bind multiple ruthenium complex ions, the signal response significantly increases, which has a wide range of applications[159−162]. Dionysiou *et al*.[159] reported a sensor using aptamers to capture microcystin-LR(MC-LR) for the removal of $Ru(NH_3)_6^{3+}$ and obtain a response signal. Based on the reason that after the aptamers bind to MC-LR, the $Ru(NH_3)_6^{3+}$ originally bound to the aptamer will be removed, resulting in the decrease of SWV peak, the reduction of $Ru(NH_3)_6^{3+}$ signal is positively correlated with the concentration. The selectivity for microcystin congeners with very similar structures and inference substances that may appear in the lake environment has been verified[Fig.4(B)]. The detection limit of the sensor is 9.2 pmol/L.

As an oligonucleotide sequence with recognition ability, aptamer itself has the hybridization ability of nucleotide sequence. When aptamers bind with their targets, the interaction between them is often greater than that of the hybridization of aptamers and their complementary chain, so the hybridization ability of nucleic acid can be used to design more diverse sensing strategies, which not only provides higher flexibility for the sensing strategies of the E-AB sensor, but also further improves the selectivity and application range of the sensor.

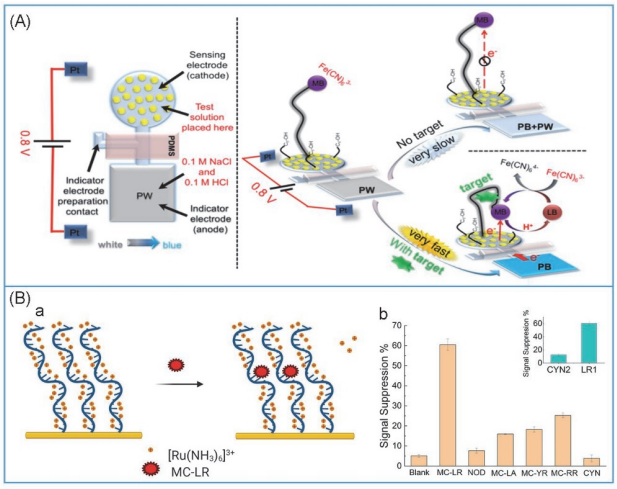

Fig.4 Sensors for small moleculars based on the electrochemical indicator

(A) Schematic illustration of the electrochemical closed-bipolar electrodes employing aptamer recognition and the detection process based on colorimetric method. Reprinted with permission from Ref.[82], Copyright 2019, American Chemical Society; (B) schematic illustation of working principle of the E-AB ensor *via* target-induced displacement of surface-confined $[Ru(NH_3)_6]^{3+}$(a), and specificity of the sensor in response to the presence of 1 nmol/L various cyanotoxins in Tris buffer(b). Reprinted with permission from Ref.[159], Copyright 2021, American Chemical Society.

Hybridization and dehybridization between nucleic acid sequences need appropriate temperature. Lin *et al*.[84] reported a sensor, which hybridizes nucleic acid by heating electrode itself rather than heating solution system. The aptamers are hybridized with the complementary chains on the electrode surface. When the target substance bisphenol A exists in the system, the aptamers are removed. Then the DNA with two hairpin structures and the fixed complementary chains form a longer dsDNA structure, which can combine with multiple electrochemiluminescence(ECL) signal substance $Ru(phen)_3^{3+}$ to generate signals. Moreover, the signal increases significantly at higher temperature[Fig.(5A)]. The detection limit of ECL method at 55 °C is 1.5 pmol/L, which is 6 times lower than that at 25 °C.

The hybridization strategies between nucleic acid chains have been flexibly applied to the fabrication of various aptamers, which is also one of the characteristics of aptamers different from other natural specific recognition molecules. De Wael *et al*.[163] used the change of the overall configuration of the aptamer after binding the target to control the hybridization between the end of the nucleic acid chain and the complementary chain modified on the electrode, and then detected testosterone by ECL method. Han *et al*.[164] reported a new complex sensor by using nanoparticles and double ring structure on the electrode surface through the combination of circular and linear nucleotides. The switch of the sensor can be controlled by adding different aptamers, and the sensor can detect the concentration of two substances[Fig.5(B)]. The detection limits of kanamycin and neomycin were 350 and 17 pmol/L, respectively. Attributed to this sensing strategy, 1000-folds interfering ions and 100-folds ascorbic acid generate less than 5% signal interference.

Based on the hybridization ability of nucleic acids, amplification strategies can be designed. Multiple-cycles amplification strategies can be used to amplify the corresponding signal of aptamers, or generate secondary targets. It is an extremely sensitive and selective sensing strategy, and the detection limit is usually down to pmol/L level, even in complex environments. Huang *et al*.[165] reported a sensing strategy using three-cycle processes to generate the DNA sequence as the secondary target. Relying on the hybridization of nucleotides and assisted by nucleic acid cleavage enzyme, the concentration signal of antibiotic can be

https://doi.org/10.1007/s40242-022-2084-z

converted to that of the secondary target. The secondary target DNA hybridizes with the one chain of dsDNA modified on the electrode surface, leaving the ssDNA modified with MB to generate signals. The detection limit of DPV method can reach 1.3 fmol/L, and the linear range is 5 fmol/L—100 pmol/L. In another example, Li *et al*.[166] used a two-cycle process to make the MB removed in the cycle with the participation of antibiotics as the target molecule to generate a signal response. Aptamers are involved in the circular process in the removal of MB, rather than directly modifying the electrode. In the absence of the target, MB binds to nucleotide chains with a hairpin structure and could not reach the electrode surface. Importantly, 25-folds concentrations of interfering substances have not generated noticeable response, highlighting the excellent selectivity of the sensor. Using DPV, the detection limit of ampicillin reaches 4.0 pmol/L[Fig.5(C)].

Combining with functional materials is also an excellent sensing strategy for the sensing of small molecules. In addition to combining with metal nanoparticles and carbon materials, such as carbon nanotubes and graphene, the sensor fabricated by combining aptamers with piezoelectric crystal materials also has excellent performance. Piezoelectric crystal material is a kind of functional materials that can generate voltage inside the crystal when pressure is applied on the surface of the crystal material. When the aptamer captures the target, the interaction with the target will lead to the change of interface

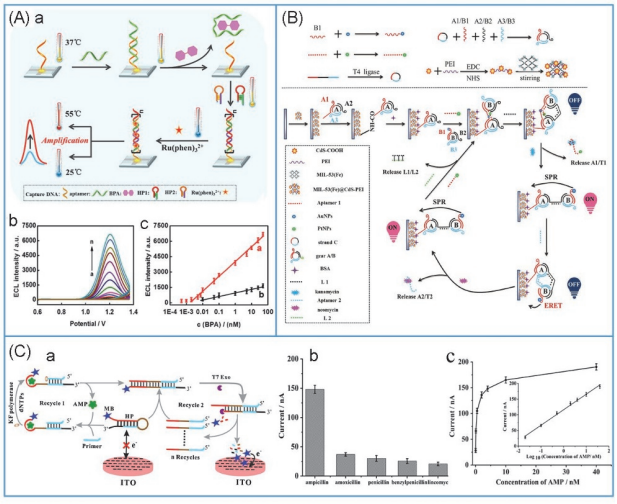

Fig.5 Sensors for small moleculars based on the hybridization

(A) Schematic illustration of the signal-on ECL aptasensor for *in situ* detection of BPA based on hybridization chain reaction and electrically heated electrode(a), ECL signals with different concentrations of BPA at the electrode temperature of 55 °C(b), and the relationship between ECL intensity and the BPA concentration at different electrode temperature of 55 and 25 °C(c). Reprinted with permission from Ref.[84], Copyright 2019, Elsevier; (B) aptamer-based sensor for the kanamycin and neomycin detection. Reprinted with permission from Ref.[164], Copyright 2019, Elsevier; (C) schematic illustration of principle of target-induced and T7 exonuclease-aided recycling amplification homogeneous electrochemical strategy for highly sensitive detection of AMP(a), DPV response of the biosensing platform in the presence of AMP and its analogues, amoxicillin, penicillin, benzylpenicillin and lincomycin, respectively(b), and the calibration curve corresponding to the DPV peak current as a function of AMP concentration at the potential of −0.3 V(c). Reprinted with permission from Ref.[166], Copyright 2016, Elsevier.

pressure, which can be transformed into electrical signals by piezoelectric materials[167−170]. Wang *et al*.[171] reported a method of detection for okadaic acid using piezoelectric materials by E-AB sensor. After the piezoelectric materials are modified with complementary chains of aptamers, they are incubated together with the mixture of okadaic acid and okadaic acid aptamers. Through competitive bonding, the signal is correlated with the concentration of okadaic acid. Finally, gold nanoparticles modified with complementary chains are used for improving conductivity and electrode surface interaction. The detection limit of this detection platform for okadaic acid is 0.26 ng/mL. In addition, the selectivity of the sensor was proved by analyzing with other three DSP toxins, and 10-folds interfering substances had no obvious interference.

3.2 Sensing of Macromolecule

The detection of macromolecules in biological systems, such as proteins and enzymes with complex structures, is also the focus of analytical chemistry. Biological macromolecules are very important in cancer detection and pathological research[172−174]. Their efficient detection is conducive to the prediction and prevention of diseases in advance. E-AB sensors can also be applied to macromolecules in biological systems with different sensing strategies[175].

Due to the size of macromolecules, complex structures may be formed on the electrode surface when aptamers capture macromolecules, which may hinder the signal response process on the electrode surface, so it is necessary to adopt appropriate strategies to amplify the signal[176−178]. Employing electrochemical indicators is an excellent strategy to enhancing the sensitivity and selectivity of E-AB sensor. Li *et al*.[179] reported a general strategy of using exonuclease to control the switching state of the sensor. Firstly, aptamer is modified on the electrode and combined with $Ru(NH_3)_6^{3+}$. After binding with the target, the exonuclease cannot decompose the aptamer due to the change of configuration, while the aptamer that does not bind to the target is decomposed. Therefore, the signal intensity of ruthenium hexamine is proportional to the concentration of the target, the interference of other substances is reduced obviously, and no significant signal was observed with 100-folds interfering substance. Using CV method, the detection limit of lysozyme is 2.0 nmol/L.

Another excellent strategy is amplifying the signals after the aptamer binding with target leaving the electrode. Yuan *et al*.[180] reported a sensor that can be used to detect miRNA-21 and human mucin 1(MUC1) protein. Firstly, the miRNA-21 starts the whole sensing process and its signal will be amplified and detected in the process behind. Then the sensor modified with primary nucleic acid chain will capture

the nanoparticle modified with complementary chains of the primary chain and the aptamer. After the MUC1 aptamers and two kinds of nucleic acid hairpin structures introduced into the system, complex structures are formed to combine with an electroactive indicator $[Ru(bpy)_2dppz]^{2+}$, generating a strong signal. When the aptamers capture the target and leave the electrode surface, the complex structures are removed simultaneously, causing a sharp reduction in the signal. Using ECL method, the detection limits of the sensor for miRNA-21 and MUC1 are 0.1 fmol/L and 2.4 fg/mL, respectively. The high selectivity of two different targets is demonstrated, and other RNA sequences and proteins do not significantly interfere with the signal response[Fig.6(A)].

When aptamers bind to macromolecular targets, it is also possible that aptamers only recognize and bind part of the macromolecules. Therefore, macromolecular substances may have multiple recognition aptamers and can form a variety of structures with aptamers[181−183]. Sandwich structure is a common sensing strategy for macromolecular targets and even bigger analytes. The principle of sandwich structure is to combine the material modified on the electrode surface with the analyte, and then attract a new aptamer, so that the analyte molecules are wrapped in it to form a structure similar to sandwich, and the signals of analytes can be detected through the change of electron transfer rate after structure change or the introduction of new catalytic or electroactive groups[184−186].

A variety of substances can participate in the construction of sandwich structure to form a stable sandwich structure. Shim *et al*.[187] reported a sandwich structure sensor assisted by magnetic force. Firstly, the aptamer was modified on the surface of the working electrode and the thrombin in the system was captured. Then, when the electromagnet of the working electrode was turned on, the magnetic nanoparticles (MNP) modified by antibody and toluidine blue B(TBO) will be close to the target, and then the auxiliary electromagnet was used to remove the magnetic nanoparticles not binding with thrombin to obtain the sandwich structure pTBA/Apt/thrombin/MNP@Ab-TBO. By detecting the current change, the detection limit of the sensor is 0.49 nmol/L. Nie *et al*.[188] also used the sandwich structure to detect thrombin. The difference is that they used two different aptamers to fabricate a new kind of sandwich structure TBA1/thrombin/TBA2-Go-RuNP. TBA2 is modified on graphene oxide attached with ruthenium nanoparticles. The detection limit of ECL method is 28.73 fmol/L[Fig.6(B)].

New technologies, such as molecular printing, can also be applied to the fabrication of sandwich structures. He *et al*.[189] reported a sensor based on molecular imprinted polymer(MIP) and aptamers. After a layer of chitosan is coated on the surface of the glassy carbon electrode, the molecular imprinting process is carried out on the surface, and the special structure

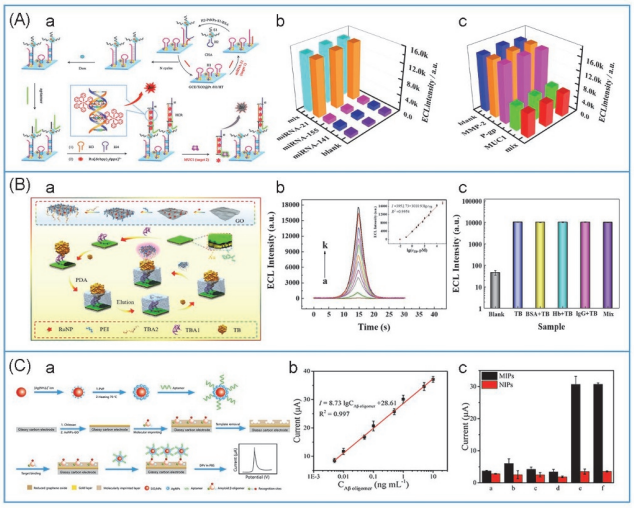

Fig.6 Sensors for macromolecular detection

(A) Schematic illustration of the versatile and ultrasensitive electrochemiluminescence biosensor for the monitoring of miRNA-21 and MUC1 from breast cancer(a), study of the selectivity performances of the biosensor for multiple types of biomarkers(b, c). Reprinted with permission from Ref.[180], Copyright 2019, American Chemical Society; (B) schematic illustration of the fabrication process of ECL aptasensor and the sandwich structure TBA1/thrombin/TBA2-Go-RuNP(a), ECL curves of the "signal-on" sensing platform to various TB concentrations(inset of the image: calibration plot of the ECL intensity and the logarithm of the TB concentrations)(b), and selectivity of the fabricated ECL sensor(c). Reprinted with permission from Ref.[188], Copyright 2021, Elsevier; (C) schematic illustration of the preparation of the SiO_2@Ag-aptamer composite, and the fabrication of the MIPs-based aptamer-based biosensor and the electrochemical detection of A-*β*O *via* a sandwich-type assay(a), the calibration curve in 0.1 mol/L PBS(pH 7.4) for detecting $A\beta_{1-42}$ oligomer at different concentrations(b), and selectivity of the MIPs biosensor in 0.1 mol/L PBS(pH 7.4) containing 1 ng/mL $A\beta$(a. $A\beta_{1-40}$ monomer, b. $A\beta_{1-42}$ monomer, c. $A\beta_{1-40}$ fibril, d. $A\beta_{1-42}$ fibril, e. $A\beta_{1-40}$ oligomer, and f. $A\beta_{1-42}$ oligomer) (c). Reprinted with permission from Ref.[189], Copyright 2020, Elsevier.

can be formed after removing the template. When there is a target in the system, the target will be embed into the imprinting layer and attract the gold nanoparticles modified with aptamers to form a sandwich structure. The results show that the selectivity and the sensitivity of the sensor are significantly enhanced by molecular printing[Fig.6(C)]. Using DPV method, the detection limit for amyloid-*β* oligomer is 1.22 pg/mL, and the linear range is 5 pg/mL—10 ng/mL.

3.3 Sensing of Cells and Viruses

Compared with macromolecules, cells and viruses are more complex organic bodies. Their efficient detection is conducive to the direct observation of the mechanism and development process of diseases, playing a great role in human health and environmental governance[66,87,139,190].

In the sensing process, cells and viruses are large, and a single aptamer is difficult to wrap the whole analyte[66,89,153]. Therefore, some strategies of macromolecular sensing cannot be directly applied to these analytes, while the selectivity and the sensitivity are still the core part of the sensor development. In this regard, sandwich structure is still a reliable method for

https://doi.org/10.1007/s40242-022-2084-z

detecting large analytes[191−194].

When sandwich structure is used in cell or virus detection, it needs to be combined with nanomaterials to improve the signal in order to obtain higher sensitivity and selectivity. Tabrizi *et al*.[97] reported a sensor for detecting adenocarcinoma gaseous cancer cell(AGS). Firstly, carbon nanotubes and primary aptamers were modified on it, capturing AGS, and then metal nanoparticles modified with secondary aptamers were immobilized. With hydrogen peroxide as a reductant, the concentration of AGS could be detected by amperometric method. The detection limit of the sensor is 6 cell/mL and the linear range is 10—5×10^5 cell/mL.

Vajhadin *et al*.[101] reported a sandwich structure that used aptamers to recognize specific proteins to capture HER2 positive cancer cells. The aptamers are dividedly modified on $CoFe_2O_4$@Ag nanoparticles and MXene material attached to the electrode to form a sandwich structure for capturing the target cancer cell. The usage of nanomaterial and MXene increases the conductivity and modification area for higher selectivity and sensitivity. Using DPV method, the detection limit is 47 cell/mL with a linear relationship in the range of 10^2—10^6 cell/mL[Fig.7(A)]. Compared with the target cells SK-BR-3 at a high expression level, other cancer cells at medium or low expression level generate basically negligible response.

As viruses and cells are complex organisms, their surfaces have many different functional structures, and they have abundant sites for aptamer recognition[89,195,196]. Therefore, multi segment of aptamers can be used to form a winding structure for analytes, which can successfully capture viruses and cells with high sensitivity and selectivity. Xiang *et al*.[89] modified the primer DNA on the surface of the gold electrode, and then formed a multivalent aptamer network for capturing the target circulating tumor cells(CTCs) with the assistance of DNA template and rolling circle amplification. After the aptamer network wrapping the CTCs, gold nanoparticles modified with antibodies will be introduced into the electrode surface as a catalyst for the H_2O_2 oxidation to generate signals. Except for the target cancer cells, other cancer cells cannot generate obvious signal responses[Fig.7(B)]. Using CV method, the detection limit of the sensor in the whole blood is 5 cell/mL. The binding and detection of aptamers with macromolecules or larger analytes require aptamers with better affinity. This can be achieved by combining multiple aptamers[197−199]. For instance, the detection of coronavirus(SARS-Cov-2) is the most concerned challenge since the outbreak of the epidemic. Efficient and rapid response to the virus is vital for biosensors in this urgent situation. Li *et al*.[200] reported an effective sensor for the detection of a new type of SARS-Cov-2 using two newly generated aptamers. The combined use of aptamers targeting MSA1T and MSA5T formed a sensor with excellent selectivity

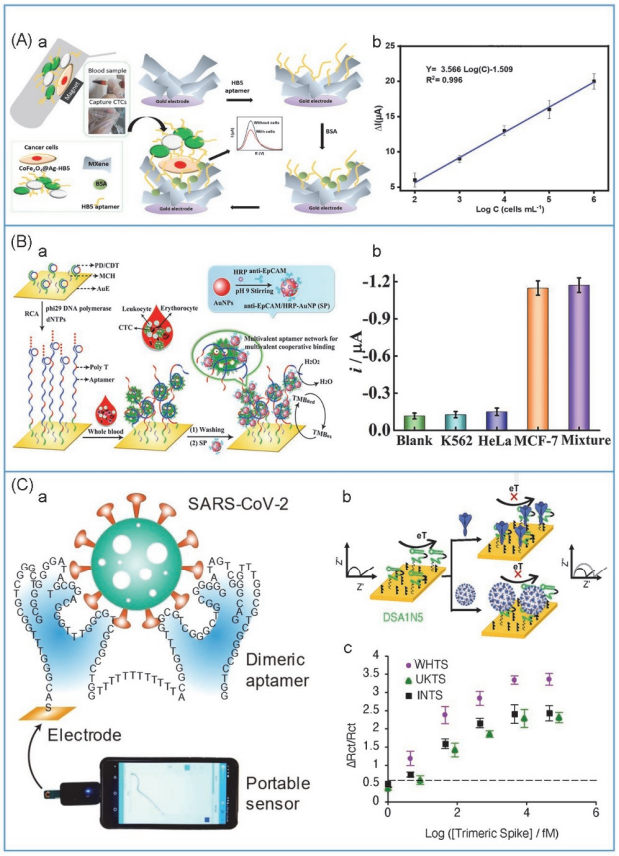

Fig.7 Sensors for the detection of cells and viruses

(A) Schematic illustration of an MXene-based cytosensor for the detection of SK-BR-3 cells(magnetic cell isolation using $CoFe_2O_4$@Ag-HB5 and electrochemical cell detection on a functionalized MXene-based surface)(a), and linear calibration curve of the current change and the logarithmic value of SK-BR-3 cell concentration(b). Reprinted with permission from Ref.[101], Copyright 2022, Elsevier; (B) schematic illustration of multivalent aptamer network for capturing and electrochemical detection of CTCs in whole blood(a), and current responses of the method for the detection of different cancer cells(5×10^3 cells/mL)(b). Reprinted with permission from Ref.[89], Copyright 2020, American Chemical Society; (C) illustration of sensor connected with portable device capturing the target virus by dimeric aptamer(a), schematic of the electrochemical assay for the detection of SARS-CoV-2 using spike protein aptamer(after incubation with the viral target, the charge transfer resistance increases due to surface blocking of the redox reaction of the Fe^{2+}/Fe^{3+} ions)(b), and calibration plot of the different concentrations of three trimeric spike proteins, WHTS, UKTS and INTS[dotted line indicates the mean signal change for the buffer without protein load(*n*=3)](c). Reprinted with permission from Ref.[200], Copyright 2021, Wiley-VCH.

for SARS-Cov-2 detection. When aptamers bound with SARS-Cov-2, the electron transfer rate on the electrode surface was blocked. Under the electrochemical impedance spectroscopy(EIS), the detection limits for Wuhan variety, British variety and Indian variety are 1, 2.8 and 3.6 fmol/L, respectively[Fig.7(C)]. More excitingly, when equipped with portable devices, the sensing results can be obtained quickly after simple treatment.

In conclusion, the sensing strategies of E-AB sensor has strong flexibility, wide application range and fast response, and can be widely used in reality to fulfill the detection tasks with high selectivity and sensitivity in complex systems(Table 2).

Table 2 Some examples of E-AB sensors

Target	Modification strategy	Method	Limit of detection	Linear range	Ref.
Adenosine	Covalent(CONH)	ECL	1 fmol/L	10^{-6}—10^{2} nmol/L	[78]
AFP	Covalent(CONH)	CV	3 pg/mL	10^{-2}—10^{2} ng/mL	[79]
	Covalent(CONH)	SWV	1.22 ng/mL	3—30 ng/mL	[80]
AGS	Covalent(Au—S)	Amperometry	6 cell/mL	10—5×10^{5} cell/mL	[97]
Ampicillin	Covalent(Au—S)	DPV	1 pmol/L	7 pmol/L—10^{2} nmol/L	[81]
	Non-modification	DPV	4 pmol/L	0.02—40 nmol/L	[165]
Amyloid-*β* oligomer	Covalent(Ag—S)	DPV	1.22 pg/mL	5×10^{-3}—10 ng/mL	[182]
ATP	Covalent(Au—S)	Colorimetric	1 mmol/L	1—16 mmol/L	[82]
	Covalent(CONH)	DPV	0.03 pmol/L	10^{-4}—10^{3} nmol/L	[108]
BPA	Covalent(Au—S)	ECL	1.5 pmol/L	2×10^{-3}—50 nmol/L	[84]
	Covalent(Au—S)	ECL	33 pmol/L	10^{-4}—40 μmol/L	[85]
Cardiac troponin I	Biotin-streptavidin strategy	DPV	100 amol/L	10^{-4}—10 pmol/L	[126]
	Biotin-streptavidin strategy	EIS	10 fmol/L	10^{-5}—1 nmol/L	[201]
Cocaine	Covalent(Au—S)	DPV	105 pmol/L	0.1—50 nmol/L	[88]
CTC	Covalent(Au—S)	CV	25 cell/mL	10^{2}—5×10^{3} cell/mL	[89]
Dexamethasone(DXN)	Covalent(Au—S)	DPV	2.12 nmol/L	2.5—10^{2} nmol/L	[90]
Digoxin	Covalent(Au—S)	SWV	0.5 ng/mL	0.5—5.0 ng/mL	[94]
H5N1	Covalent	FET[a]	5.9 pmol/L	10^{-2}—10 nmol/L	[153]
HER2-positive cancer cells	Covalent(CONH)	DPV	47 cell/mL	10^{2}—10^{6} cell/mL	[101]
HIV-1 Tat protein	Covalent(Au—S)	QCM[b]	0.25 ppm	0.25—2.5 ppm	[92]
Kanamycin	Covalent(Au—S)	DPV	1.3 fmol/L	5×10^{-3}—10^{2} pmol/L	[166]
	Non-covalent	DPV	29 pmol/L	0.1—10^{2} nmol/L	[129]
	Covalent(Au—S)	DPV	36 fmol/L	5×10^{-2}—2×10^{2} pmol/L	[91]
	Non-covalent	ECL	0.12 nmol/L	1—206 nmol/L	[202]
Kanamycin	Covalent(CONH)	ECL	0.35 nmol/L	1—10^{4} pmol/L	[164]
Neomycin			17 pmol/L	0.1—10^{3} nmol/L	
Lysozyme	Covalent	CV	2.0 nmol/L	2.0—60 nmol/L	[179]
MALAT1	Covalent(Au—S)	DPV	42.8 fmol/L	10^{-5}—10 nmol/L	[102]
MERS-CoV	Covalent(CONH)	SERS[c]	0.525 pg/mL(SERS)	10^{-3}—10^{2} ng/mL	[203]
			0.645 pg/mL(EIS)		
Microcystin-LR	Covalent(Au—S)	SWV	9.2 pmol/L	0.03—1 nmol/L	[159]
MUC1	Covalent(Au—S)	ECL	2.4 fg/mL	10^{-5}—1 μg/mL	[180]
Okadaic acid	Covalent(Au—S)	QCM	0.32 μmol/L	0.40—160 μmol/L	[199]
PDCF-BB	Covalent(Au—S)	LSV[d]	10 fmol/L	10^{-2}—10^{2} pmol/L	[204]
SARS-CoV-2	Covalent(Au—S)	EIS	1 fmol/L	4×10^{-3}—4.4 pmol/L	[200]
Tenofovir(TFV)	Covalent(Au—S)	EIS	1.2 nmol/L	1—10^{2} nmol/L	[110]
Testosterone	Biotin-streptavidin strategy	ECL	0.29 μmol/L	0.39—1.56 μmol/L	[163]
Thrombin	Covalent(Au—S)	CC[e]	1 fmol/L	10^{-3}—1 pmol/L	[103]
	Covalent(CONH)	ECL	28.73 fmol/L	10^{-4}—10 nmol/L	[181]
	Covalent(Au—S)	DPV	0.32 pmol/L	1×10^{-3}—30 nmol/L	[205]
	Covalent(Au—S)	Amperometry	1 fmol/L	10^{-6}—10 nmol/L	[206]
Tobramycin	Covalent(Au—S)	SWV	0.51 μmol/L	0.02—0.5 μmol/L	[207]

a. FET: field effect transistor; *b*. QCM: quartz crystal microbalance; *c*. SERS: surface-enhanced Raman spectroscopy; *d*. LSV: linear sweep voltammetry.

4 Summary and Outlook

E-AB sensor features the dual advantages of aptamers and electrochemical methods, and continues to surprise and perplex scientists. Today, with the great advancement of SELEX technique, rich chemical tools for surface engineering, and controllable fabrication of electronic sensing device, microsized, portable and even wireless E-AB sensors targeting previously challenging analytes have been emerged. This greatly expands the application scope of sensors from initial *in vitro* sensing to now *in vivo* sensing, from environment analysis to human healthy monitoring, including in the diagnosis of diabetes cancer, degenerative diseases, and many others. Looking forward, in order to develop more reliable E-AB sensors for practical applications, perhaps chemists should focus on the following aspects in the future:

a) Miniaturization for *in vivo* detection. To minimize the invasiveness to living body during the implanting process of sensors, micro or even nano-sized electrochemical sensor is an appealing choice, but the decreasing modification area and special properties caused by the size effect pose grand challenges to E-AB sensors. Therefore, the effective

https://doi.org/10.1007/s40242-022-2084-z

modification of aptamers on micro electrodes, such as wire electrode, fiber electrode and so on, and developing reliable sensing strategies to achieve high sensitivity and selectivity for *in vivo* measurement are urgent problems to be solved.

b) Improving the *in vivo* stability of E-AB sensors. Effective sensing of biochemical substances *in vivo* requires the sensor to be applied in the flowing tissue fluid, for example, in cerebrospinal fluid and blood, and the complexity of fluid properties and co-existing of a large amount of other biological substances will affect the stability and selectivity of E-AB sensors. Designing bio-compatible and antifouling electrode surface to minimize the immune response of the sensor, and avoiding the degradation of aptamer in complex bio-environment can prolong the effective usage of the sensor and realize continuous sensing.

c) Large-scale production of E-AB sensors. Controlling and large-scale fabrication of E-Abs sensors with low cost can greatly boost the application of the sensor in real life, for example, applied to clinical usage for daily tracking of long-lasting health conditions for effective intervention and treatment. Compared with the commercial glucose sensor and biological oxygen sensor developed in early years, E-AB sensors need more chemical and electronic strategies for improving the large-scale synthesis of nucleic acids, interfacing the sensor with standard electronic manufacturing procedures, and avoiding the decomposing of aptamers or minimizing the batch to batch variation during the production and transportation of sensors.

Finally, we expect E-AB sensors to achieve breakthroughs in sensitivity and selectivity, and to be applied in real situations on a large scale, so as to create greater value for life and health of human beings and be sustainable development of the environment.

Acknowledgements

This work was supported by the National Natural Science Foundation of China(No.22104006), the Beijing Nova Program of Science and Technology, China(No.Z191100001119108) and the Fund of Beijing National Laboratory for Molecular Sciences, China(No.BNLMS202009).

Conflicts of Interest

The authors declare no conflicts of interest.

References

[1] Hulanicki A., Glab S., Ingman F., *Pure Appl. Chem.*, **1991**, *63*, 1247
[2] Justino C. I. L., Duarte A. C., Santos T. A. P. R., *Trends Analyt. Chem.*, **2016**, *85*, 36
[3] Matsuda M., Terai K., *Pathol. In.*, **2020**, *70*, 379
[4] Wang M. X., Li L. Y., Zhang L. M., Zhao J. G., Jiang Z. Q., Wang W. Z., *Anal. Chem.*, **2022**, *94*, 431
[5] Kirsch J., Siltanen C., Zhou Q., Revzin A., Simonian A., *Chem. Soc. Rev.*, **2013**, *42*, 8733
[6] Siontorou C. G., Georgopoulos K. N., *Trends Environ. Anal. Chem.*, **2021**, *32*, e00146
[7] Zhu Y., Zhang Q., Li X., Pan H., Wang J. T., Zhao Z. J., *Sens. Actuators B Chem.*, **2019**, *293*, 53
[8] Tu J. B., Rodriguez R. M. T., Wang M. Q., Gao W., *Adv. Funct. Mater.*, **2020**, *30*, 1906713
[9] Qi X., Wang S. Y., Jiang Y., Liu P. P., Li Q. C., Hao W., Han J. B., Zhou Y. X., Huang X., Liang P., *Water Res.*, **2021**, *198*, 117164
[10] Kalimuthu P., Kruse T., Bernhardt P. V., *Electrochim. Acta*, **2021**, *386*, 138480
[11] Ronkainen N. J., Halsall H. B., Heineman W. R., *Chem. Soc. Rev.*, **2010**, *39*, 1747
[12] Ramanathan K., Danielsson B., *Biosens. Bioelectron.*, **2001**, *16*, 417
[13] Lei Z. L., Guo B., *Adv. Sci.*, **2022**, *9*, 2102924
[14] Kauffmann J. M., Guilbault G. G., *Methods Biochem. Anal.*, **1992**, *36*, 63
[15] Therriault D., *Nat. Nanotechnol.*, **2007**, *2*, 393
[16] Turner A. P. F., *Chem. Soc. Rev.*, **2013**, *42*, 3184
[17] Mokhtarzadeh A., Eivazzadeh Keihan R., Pashazadeh P., Hejazi M., Gharaatifar N., Hasanzadeh M., Baradaran B., de la Guardia M., *Trends Analyt. Chem.*, **2017**, *97*, 445
[18] Inda M. E., Lu T. K., *Annu. Rev. Microbiol.*, **2020**, *74*, 337
[19] Bollella P., Katz E., *Sensors*, **2020**, *20*, 3517
[20] Kwon O. S., Song H. S., Park T. H., Jang J., *Chem. Rev.*, **2019**, *119*, 36
[21] Zhu C. Z., Yang G. H., Li H., Du D., Lin Y. H., *Anal. Chem.*, **2015**, *87*, 230
[22] Sempionatto J. R., Montiel V. R. V., Vargas E., Teymourian H., Wang J., *ACS Sens.*, **2021**, *6*, 1745
[23] Baldo T. A., de Lima L. F., Mendes L. F., de Araujo W. R., Paixao T. R. L. C., Coltro W. K. T., *ACS Appl. Electron. Mater.*, **2021**, *3*, 68
[24] Paniel N., Baudart J., Hayat A., Barthelmebs L., *Methods*, **2013**, *64*, 229
[25] Zhou W., Huang P. J. J., Ding J., Liu J., *Analyst*, **2014**, *139*, 2627
[26] Toh S. Y., Citartan M., Gopinath S. C. B., Tang T. H., *Biosens. Bioelectron.*, **2015**, *64*, 392
[27] Labib M., Sargent E. H., Kelley S. O., *Chem. Rev.*, **2016**, *116*, 9001
[28] Muzyka K., Saqib M., Liu Z., Zhang W., Xu G., *Biosens. Bioelectron.*, **2017**, *92*, 241
[29] Yang F., Li Q., Wang L., Zhang G. J., Fan C., *ACS Sens.*, **2018**, *3*, 903
[30] Sameiyan E., Bagheri E., Ramezani M., Alibolandi M., Abnous K., Taghdisi S. M., *Biosens. Bioelectron.*, **2019**, *143*, 111662
[31] Zhang K., Li H. Y., Wang W. J., Cao J. X., Gan N., Han H. Y., *ACS Sens.*, **2020**, *5*, 3721
[32] Jiang Z. W., Zhao T. T., Li C. M., Li Y. F., Huang C. Z., *ACS Appl. Mater. Interfaces*, **2021**, *13*, 49754
[33] An J. E., Kim K. H., Park S. J., Seo S. E., Kim J., Ha S., Bae J., Kwon O. S., *ACS Sens.*, **2022**, *7*, 99
[34] Ellington A. D., Szostak J. W., *Nature*, **1990**, *346*, 818
[35] Robertson D. L., Joyce G. F., *Nature*, **1990**, *344*, 467
[36] Gold L., *J. Biol. Chem.*, **1995**, *270*, 13581
[37] Tuerk C., Gold L., *Science*, **1990**, *249*, 505
[38] Singer B. S., Shtatland T., Brown D., Gold L., *Nucleic Acids Res.*, **1997**, *25*, 781
[39] Gopinath S. C. B., *Anal. Bioanal. Chem.*, **2007**, *387*, 171
[40] Keefe A. D., Cload S. T., *Curr. Opin. Chem. Biol.*, **2008**, *12*, 448
[41] Jayasena S. D., *Clin. Chem.*, **1999**, *45*, 1628
[42] Ilgu M., Nilsen Hamilton M., *Analyst*, **2016**, *141*, 1551
[43] Rothlisberger P., Hollenstein M., *Adv. Drug Del. Rev.*, **2018**, *134*, 3
[44] Wu Y., Belmonte I., Sykes K. S., Xiao Y., White R. J., *Anal. Chem.*, **2019**, *91*, 15335
[45] Kleinjung F., Klussmann S., Erdmann V. A., Scheller F. W., Furste J. P., Bier F. F., *Anal. Chem.*, **1998**, *70*, 328
[46] Xiao Y., Piorek B. D., Plaxco K. W., Heeger A. J., *J. Am. Chem. Soc.*, **2005**, *127*, 17990
[47] Du Y., Li B. L., Wang E. K., *Acc. Chem. Res.*, **2013**, *46*, 203
[48] Zhang Y., Lai B. S., Juhas M., *Molecules*, **2019**, *24*, 941
[49] Wang L., Xu M., Han L., Zhou M., Zhu C. Z., Dong S. J., *Anal. Chem.*, **2012**, *84*, 7301
[50] Ma K., Li X., Xu B., Tian W. J., *Anal. Chim. Acta*, **2021**, *1188*, 338859
[51] Nekrasov N., Jaric S., Kireev D., Emelianov A. V., Orlov A. V., Gadjanski I., Nikitin P. I., Akinwande D., Bobrinetskiy I., *Biosens. Bioelectron.*, **2022**, *200*, 113890
[52] Chai S. C., Cao X., Xu F. R., Zhai L., Qian H. J., Chen Q., Wu L. X., Li H. L., *ACS Nano*, **2019**, *13*, 7135
[53] Wang Y., Gong C. J., Zhu Y., Wang Q. Q., Geng L. P., *Electrochim. Acta*, **2021**, *393*, 139054
[54] Rahmati Z., Roushani M., Hosseini H., *Talanta*, **2022**, *237*, 122924
[55] Hori S., Herrera A., Rossi J. J., Zhou J., *Cancers*, **2018**, *10*, 9
[56] Omer M., Andersen V. L., Nielsen J. S., Wengel J., Kjems J., *Mol. Ther. Nucleic Acids*, **2020**, *22*, 994
[57] Shigdar S., Schrand B., Giangrande P. H., de Franciscis V., *Mol. Ther.*, **2021**, *29*, 2396
[58] Chen K., Liu B., Yu B., Zhong W., Lu Y., Zhang J. N., Liao J., Liu J., Pu Y., Qiu L. P., Zhang L. Q., Liu H. X., Tan W. H., *Wiley Interdiscip. Rev. Nanomed. Nanobiotechnol.*, **2017**, *9*, e1438

[59] Fattal E., Hillaireau H., Ismail S. I., *Adv. Drug Del. Rev.*, **2018**, *134*, 1
[60] Gunaratne R., Kumar S., Frederiksen J. W., Stayrook S., Lohrmann J. L., Perry K., Bompiani K. M., Chabata C. V., Thalji N. K., Ho M. D., Arepally G., Camire R. M., Krishnaswamy S., Sullenger B. A., *Nat. Biotechnol.*, **2018**, *36*, 606
[61] Gooch J., Daniel B., Parkin M., Frascione N., *Trends Analyt. Chem.*, **2017**, *94*, 150
[62] Aydindogan E., Balaban S., Evran S., Coskunol H., Timur S., *Biosensors*, **2019**, *9*, 118
[63] Satoh T., Kouroki S., Kitamura Y., Ihara T., Matsumura K., Iwase S., *Anal. Methods*, **2020**, *12*, 2703
[64] Dunn M. R., Jimenez R. M., Chaput J. C., *Nat. Rev. Chem.*, **2017**, *1*, 1
[65] Keefe A. D., Pai S., Ellington A., *Nat. Rev. Drug Discov.*, **2010**, *9*, 537
[66] Wu L. L., Wang Y. D., Xu X., Liu Y. L., Lin B. Q., Zhang M. X., Zhang J. L., Wan S., Yang C. Y., Tan W. H., *Chem. Rev.*, **2021**, *121*, 12035
[67] Thevenot D. R., Toth K., Durst R. A., Wilson G. S., *Anal. Lett.*, **2001**, *34*, 635
[68] Ikebukuro K., Kiyohara C., Sode K., *Biosens. Bioelectron.*, **2005**, *20*, 2168
[69] Xue Y. F., Ji W. L., Jiang Y., Yu P., Mao L. Q., *Angew. Chem. Int. Ed.*, **2021**, *60*, 23777
[70] Jolly P., Miodek A., Yang D. K., Chen L. C., Lloyd M. D., Estrela P., *ACS Sens.*, **2016**, *1*, 1308
[71] Wang G. X., Han R., Li Q., Han Y. F., Luo X. L., *Anal. Chem.*, **2020**, *92*, 7186
[72] Su S., Ma J. F., Xu Y. Q., Pan H. M., Zhu D., Chao J., Weng, L. X., Wang L. H., *ACS Appl. Mater. Interfaces*, **2020**, *12*, 48133
[73] Bang G. S., Cho S., Kim B. G., *Biosens. Bioelectron.*, **2005**, *21*, 863
[74] Odeh F., Nsairat H., Alshaer W., Ismail M. A., Esawi E., Qaqish B., Al Bawab A., Ismail S. I., *Molecules*, **2020**, *25*, 3
[75] Feigon J., Dieckmann T., Smith F. W., *Chem. Biol.*, **1996**, *3*, 611
[76] Piganeau N., Schroeder R., *Chem. Biol.*, **2003**, *10*, 103
[77] Ruff K. M., Snyder T. M., Liu D. R., *J. Am. Chem. Soc.*, **2010**, *132*, 9453
[78] Shi H. W., Wu M. S., Du Y., Xu J. J., Chen H. Y., *Biosens. Bioelectron.*, **2014**, *55*, 459
[79] Yang S. H., Zhang F. F., Wang Z. H., Liang Q. L., *Biosens. Bioelectron.*, **2018**, *112*, 186
[80] Upan J., Youngvises N., Tuantranont A., Karuwan C., Banet P., Aubert P. H., Jakmunee J., *Sci. Rep.*, **2021**, *11*, 1
[81] Taghdisi S. M., Danesh N. M., Nameghi M. A., Rarnezani M., Alibolandi M., Abnous K., *Biosens. Bioelectron.*, **2019**, *133*, 230
[82] Zhang X., Lazenby R. A., Wu Y., White R. J., *Anal. Chem.*, **2019**, *91*, 11467
[83] Tivon Y., Falcone G., Deiters A., *Angew. Chem. Int. Ed.*, **2021**, *60*, 15899
[84] Zhang H. F., Luo F., Wang P. L., Guo L. H., Qiu B., Lin Z. Y., *Biosens. Bioelectron.*, **2019**, *129*, 36
[85] Liu X. H., Luo L. J., Li L. B., Di Z. X., Zhang J. Y., You T. Y., *Electrochim. Acta*, **2019**, *319*, 849
[86] Adachi T., Nakamura Y., *Molecules*, **2019**, *24*, 4229
[87] Ni S. J., Zhuo Z. J., Pan Y. F., Yu Y. Y., Li F. F., Liu J., Wang L. Y., *ACS Appl. Mater. Interfaces*, **2021**, *13*, 9500
[88] Taghdisi S. M., Danesh N. M., Emrani A. S., Ramezani M., Abnous K., *Biosens. Bioelectron.*, **2015**, *73*, 245
[89] Yang J. M., Li X. L., Jiang B. Y., Yuan R., Xiang Y., *Anal. Chem.*, **2020**, *92*, 7893
[90] Mehennaoui S., Poorahong S., Jimenez G. C., Siaj M., *Sci. Rep.*, **2019**, *9*, 1
[91] Zeng R. J., Su L. S., Luo Z. B., Zhang L. J., Lu M. H., Tang D. P., *Anal. Chim. Acta*, **2018**, *1038*, 21
[92] Minunni M., Tombelli S., Gullotto A., Luzi E., Mascini M., *Biosens. Bioelectron.*, **2004**, *20*, 1149
[93] Zamani M., Robson J. M., Fan A., Bono M. S., Furst A. L., Klapperich C. M., *ACS Cent. Sci.*, **2021**, *7*, 963
[94] Yu H., Chen Z., Liu Y., Alkhamis O., Song Z., Xiao Y., *Angew. Chem. Int. Ed.*, **2021**, *60*, 2993
[95] Wang J., Zhou H. S., *Anal. Chem.*, **2008**, *80*, 7174
[96] Huang K. J., Liu Y. J., Zhang J. Z., Cao J. T., Liu Y. M., *Biosens. Bioelectron.*, **2015**, *67*, 184
[97] Tabrizi M. A., Shamsipur M., Saber R., Sarkar S., Sherkatkhameneh N., *Electrochim. Acta*, **2017**, *246*, 1147
[98] Qiang L., Zhang Y., Guo X., Gao Y. K., Han Y., Sun J., Han L., *RSC Adv.*, **2020**, *10*, 15293
[99] Zhang C. Y., Wang C. W., Xiao R., Tang L, Huang J, Wu D, Liu S. W., Wang Y., Zhang D., Wang S. Q., Chen X. M., *J. Mater. Chem B*, **2018**, *6*, 3751
[100] Chen M., Wu D. M., Tu S. H., Yang C. Y., Chen D. J., Xu Y., *Sci. Rep.*, **2021**, *11*, 3666
[101] Vajhadin F., Mazloum Ardakani M., Shahidi M., Moshtaghioun S. M., Haghiralsadat F., Ebadi A., Amini A., *Biosens. Bioelectron.*, **2022**, *195*, 113626
[102] Cheng S. T., Liu H. M., Zhang H., Chu G. L., Guo Y. M., Sun X., *Sens. Actuators B Chem.*, **2020**, *304*, 127367
[103] Malecka K., Ferapontova E. E., *ACS Appl. Mater. Interfaces*, **2021**, *13*, 37979
[104] Azadbakht A., Roushani M., Abbasi A. R., Derikvand Z., *Anal. Biochem.*, **2016**, *507*, 47
[105] Azadbakht A., Roushani M., Abbasi A. R., Derikvand Z., *Anal. Biochem.*, **2016**, *512*, 58
[106] Raouafi A., Sanchez A., Raouafi N., Villalonga R., *Sens. Actuators B Chem.*, **2019**, *297*, 126762
[107] Jia F., Duan N., Wu S. J., Dai R. T., Wang Z. P., Li X. M., *Mikrochim. Acta*, **2016**, *183*, 337
[108] Li Z. J., Yin J. F., Gao C. H., Sheng L. Y., Meng A., *Mikrochim. Acta*, **2019**, *186*, 1
[109] Li J. J., Si Y. P., Park Y. E, Choi J., Jung S. M., Lee J. E., Lee H. Y., *Mikrochim. Acta*, **2021**, *188*, 146
[110] Szymczyk A., Soliwodzka K., Moskal M., Rozanowski K., Ziolkowski R., *Sens. Actuators B: Chem.*, **2022**, *354*, 131086
[111] Ma Y. B., Liu J. S., Li H. D., *Biosens. Bioelectron.*, **2017**, *92*, 21
[112] Ding S., Mosher C., Lee X. Y., Das S. R., Cargill A. A., Tang X., Chen B., McLamore E. S., Gomes C., Hostetter J. M., Claussen J. C., *ACS Sens.*, **2017**, *2*, 210
[113] Xiao Q., Feng J. R., Li J. W., Feng M. M., Huang S., *Analyst*, **2018**, *143*, 4764
[114] Meng X. Z., Gu H. W., Yi H. C., He Y. Q., Chen Y., Sun W. Y., *Anal. Chim. Acta*, **2020**, *1125*, 1
[115] Liu X. P., Huang B., Mao C. J., Chen J. S., Jin B. K., *Talanta*, **2021**, *233*, 122546
[116] Xu X. X., Makaraviciute A., Kumar S., Wen C. Y., Sjodin M., Abdurakhmanov E., Danielson U. H., Nyholm L., Zhang Z., *Anal. Chem.*, **2019**, *91*, 14697
[117] Aliakbarinodehi N., Jolly P., Bhalla N., Miodek A., De Micheli G., Estrela P., Carrara S., *Sci. Rep.*, **2017**, *7*, 1
[118] Li Y. F., Liu L. L., Fang X. L., Bao J. C., Han M., Dai Z. H., *Electrochim. Acta*, **2012**, *65*, 1
[119] Wang Y. F., Sha H. F., Ke H., Xiong X., Jia N. Q., *Electrochim. Acta*, **2018**, *290*, 90
[120] Pur M. R. K., Hosseini M., Faridbod F., Ganjali M. R., Hosseinkhani S., *Sens. Actuators B Chem.*, **2018**, *257*, 87
[121] Li Y., Han R., Chen M., Zhang L. Y., Wang G. X., Luo X. L., *Anal. Chem.*, **2021**, *93*, 4326
[122] Lasserre P., Balansethupathy B., Vezza V. J., Butterworth A., Macdonald A., Blair E. O., McAteer L., Hannah S., Ward A. C., Hoskisson P. A., Longmuir A., Setford S., Farmer E. C. W., Murphy M. E., Flynn H., Corrigan D. K., *Anal. Chem.*, **2022**, *94*, 2126
[123] Yasun E., Li C., Barut I., Janvier D., Qiu L. P., Cui C., Tan W. H., *Nanoscale*, **2015**, *7*, 10240
[124] Klose A. M., Miller B. L., *Sensors*, **2020**, *20*, 5745
[125] Izrailev S., Stepaniants S., Balsera M., Oono Y., Schulten Y., *Biophys. J.*, **1997**, *72*, 1568
[126] Zhang J. T., Lakshmipriya T., Gopinath S. C. B., *ACS Omega*, **2020**, *5*, 25899
[127] Ming T., Cheng Y., Xing Y., Luo J. P., Mao G., Liu J. T., Sun S., Kong F. L., Jin H. Y., Cai X. X., *ACS Appl. Mater. Interfaces*, **2021**, *13*, 46317
[128] Zhang Y., Zheng B., Zhu C. F., Zhang X., Tan C. L., Li H., Chen B., Yang J. Z., Chen J., Huang Y., Wang L. H., Zhang H., *Adv. Mater.*, **2015**, *27*, 935
[129] Zhou Y. L., Li F., Wu H. W., Chen Y., Yin H. S., Ai S. Y., Wang J., *Sens. Actuators B Chem.*, **2019**, *296*, 126664
[130] Hou H. F., Jin Y., Wei H., Ji W. L., Xue Y. F., Hu J. B., Zhang M. N., Jiang Y., Mao L. Q., *Angew. Chem. Int. Ed.*, **2020**, *59*, 18996
[131] Khan S., Burciu B., Filipe C. D. M., Li Y., Dellinger K., Didar T. F., *ACS Nano*, **2021**, *15*, 13943
[132] Zhang W., Wang L., Yang Y. S., Gaskin P., Teng K. S., *ACS Sens.*, **2019**, *4*, 1138
[133] Rayappa M. K., Viswanathan P. A., Rattu G., Krishna P. M., *J. Agric. Food Chem.*, **2021**, *69*, 4578
[134] Jin Y., Li X., Jiang Y., *Chem. Nano. Mat.*, **2021**, *7*, 489
[135] Erfani A., Seaberg J., Aichele C. P., Ramsey J. D., *Biomacromolecules*, **2020**, *21*, 2557
[136] Madhurantakam S., Karnam J. B., Brabazon D., Takai M., Ul Ahad I., Rayappan J. B. B., Krishnan U. M., *ACS Chem. Neurosci.*, **2020**, *11*, 4024
[137] Somerson J., Plaxco K. W., *Molecules*, **2018**, *23*, 912
[138] Jin J., Ji W. L., Li L. J., Zhao G., Wu W. J., Wei H., Ma F. R., Jiang Y., Mao L. Q., *J. Am. Chem. Soc.*, **2020**, *142*, 19012
[139] Yu H. X., Alkhamis O., Canoura J., Liu Y. Z., Xiao Y., *Angew. Chem. Int. Ed.*, **2021**, *60*, 16800
[140] Shen M. M., Kan X. W., *Electrochim. Acta*, **2021**, *367*, 137433
[141] Walsh R., Ho U., Wang X. L., DeRosa M. C., *Can. J. Chem.*, **2015**, *93*, 572
[142] Talemi R. P., Mousavi S. M., Afruzi H., *Mater. Sci. Eng. for Biological*

Applications, **2017**, *73*, 700
[143] Tabb J., Rapoport E., Han I., Lombardi J., Green O., *Nanomedicine*, **2022**, *41*, 102528
[144] Liu X. X., Liu J. W., *View*, **2021**, *2*, 20200102
[145] Jin H., Zhao C. Q., Gui R. J., Gao X. H., Wang Z. H., *Anal. Chim. Acta*, **2018**, *1025*, 154
[146] Liu S., Xing X. R., Yu J. H., Lian W. J., Li J, Cui M., Huang J. D., *Biosens. Bioelectron.*, **2012**, *36*, 186
[147] Wang W. T., Wang W., Davis J. J., Luo X. L., *Mikrochim. Acta*, **2015**, *182*, 1123
[148] Martos I. A., Moller A., Ferapontova E. E., *ACS Chem. Neurosci.*, **2019**, *10*, 1706
[149] Zhou J. W., Wang W. Y., Yu P., Xiong E. H., Zhang X. H., Chen J. H., *RSC Adv.*, **2014**, *4*, 52250
[150] Taheri R. A., Eskandari K., Negandary M., *Microchem. J.*, **2018**, *143*, 243
[151] Sui C. J., Zhou Y. L., Wang M. Y., Yin H. S., Wang P., Ai S. Y., *Sens. Actuators B: Chem.*, **2018**, *266*, 514
[152] Wu L. D., Xu Z. Y., Meng Q. Y., Xiao Y. S., Cao Q., Rathi B. Liu H., Han G., Zhang J., Yan J., *Anal. Chim. Acta*, **2020**, *1099*, 39
[153] Kwon J., Lee Y., Lee T., Ahn J. H., *Anal. Chem.*, **2020**, *92*, 5524
[154] Wang C., Zhao Q., *Biosens. Bioelectron.*, **2020**, *167*, 112478
[155] Miao X. M., Li Z. B., Zhu A. H., Feng Z. Z., Tian J., Peng X., *Biosens. Bioelectron.*, **2016**, *83*, 39
[156] Geng X., Zhang M. T., Long H. Y., Hu Z. H., Zhao B. Y., Feng L. Y., Du J. Y., *Anal. Chim. Acta*, **2021**, *1145*, 124
[157] Ren Q., Mou J. S., Guo Y. M., Wang H. Q., Cao X. Y., Zhang F. F., *Biosens. Bioelectron.*, **2020**, *166*, 112448
[158] Jin H., Gui R. J., Gao X. H., Sun Y. J., *Biosens. Bioelectron.*, **2019**, *145*, 111732
[159] Vogiazi V., de la Cruz A. A., Varughese E. A., Heineman W. R., White R. J., Dionysiou D. D., *ACS ES&T Eng.*, **2021**, *1*, 1597
[160] Tabrizi M. A., Shamsipur M., Saber R., Sarkar S., Ebrahimi V., *Biosens. Bioelectron.*, **2017**, *98*, 113
[161] Ma C., Liu H. Y., Zhang L. N., Li H., Yan M., Song X. R., Yu J. H., *Biosens. Bioelectron.*, **2018**, *99*, 8
[162] Xing Y. C., Chen X. X., Jin B. X., Chen P. P., Huang C. B., Jin Z. G., *Langmuir*, **2021**, *37*, 3612
[163] Canovas R., Daems E., Campos R., Schellinck S., Madder A., Martins J. C., Sobott F., De Wael K., *Talanta*, **2022**, *239*, 123121
[164] Feng D. F., Tan X. C., Wu Y. Y., Ai C. H., Luo Y. N., Chen Q.Y., Han H. Y., *Biosens. Bioelectron.*, **2019**, *129*, 100
[165] Wang H. Z., Wang Y., Liu S., Yu J. H., Guo Y. N., Xu Y., Huang J. D., *Biosens. Bioelectron.*, **2016**, *80*, 471
[166] Wang X., Dong S., Gai P., Duan R., Li F., *Biosens. Bioelectron.*, **2016**, *82*, 49
[167] Starr M. B., Shi J., Wang X. D., *Angew. Chem. Int. Ed.*, **2012**, *51*, 5962
[168] Chorsi M. T., Curry E. J., Chorsi H. T., Das R., Baroody J., Purohit P. K., Ilies H., Nguyen T. D., *Adv. Mater.*, **2019**, *31*, 1802084
[169] Qian W. Q., Yang W. Y., Zhang Y., Bowen C. R., Yang Y., *Nanomicro Lett.*, **2020**, *12*, 149
[170] Mahapatra S. D., Mohapatra P. C., Aria A. I., Christie G., Mishra Y. K., Hofmann S., Thakur V. K., *Adv. Sci.*, **2021**, *8*, 2100864
[171] Tian Y. L., Zhu P., Chen Y. T., Bai X. Y., Du L. P., Chen W., Wu C. S., Wang P., *Sens. Actuators B Chem.*, **2021**, *346*, 130446
[172] Fernandez Leiro R., Scheres S. H. W., *Nature*, **2016**, *537*, 339
[173] Singh S., Halder A., Sinha O., Chakrabarty N., Chatterjee T., Adhikari A., Singh P., Shikha D., Ghosh R., Banerjee A., Das Mahapatra P. P., Mandhar A., Bhattacharyya M., Bose S., Ahmed S. A., Alharbi A., Hameed A. M., Pal S. K., *Front. Oncol.*, **2020**, *10*, 529132
[174] Li F. Q., Yang W. Q., Zhao B. R., Yang S., Tang Q. Y., Chen X. J., Dai H. L., Liu P., *Adv. Sci.*, **2022**, *9*, 2102804
[175] Han K., Liu T., Wang Y. H., Miao P., *Rev. Anal. Chem*, **2016**, *35*, 201
[176] Famulok M., Mayer G., *Acc. Chem. Res.*, **2011**, *44*, 1349
[177] Song K. M., Lee S., Ban C., *Sensors*, **2012**, *12*, 612
[178] Citartan M., Ch'ng E. S., Rozhdestvensky T. S., Tang T. H., *Microchem. J.*, **2016**, *128*, 187
[179] Gao X. Y., Qi L., Liu K., Meng C. C., Li Y. C., Yu H. Z., *Anal. Chem.*, **2020**, *92*, 6229
[180] Nie Y. M., Yuan X. D., Zhang P., Chai Y. Q., Yuan R., *Anal. Chem.*, **2019**, *91*, 3452
[181] Yuce M., Ullah N., Budak H., *Analyst*, **2015**, *140*, 5379
[182] Chen A. L., Yan M. M., Yang S. M., *Trends Analyt. Chem.*, **2016**, *80*, 581
[183] Wang T., Chen C. Y., Larcher L. M., Barrero R. A., Veedu R. N., *Biotechnol. Adv.*, **2019**, *37*, 28
[184] Shen J. W., Li Y. B., Gu H. S., Xia F., Zuo X. L., *Chem. Rev.*, **2014**, *114*, 7631
[185] Yoon S., Rossi J. J., *Adv. Drug Del. Rev.*, **2018**, *134*, 22
[186] Debiais M., Lelievre A., Smietana M., Mueller S., *Nucleic Acids Res.*, **2020**, *48*, 3400
[187] Chung S., Moon J. M., Choi J., Hwang H., Shim Y. B., *Biosens. Bioelectron.*, **2018**, *117*, 480
[188] Yang C. N., Tian Y., Wang B. Y., Guo Q. F., Nie G. M., *Sens. Actuators B Chem.*, **2021**, *338*, 129870
[189] You M., Yang S., An Y., Zhang F., He P. G., *J. Electroanal. Chem.*, **2020**, *862*, 114017
[190] Asdaq S. M. B., Ikbal A. M. A., Sahu R. K., Bhattacharjee B., Paul T., Deka B., Fattepur S., Widyowati R., Vijaya J., Al Mohaini M., Alsalman A. J., Imran M., Nagaraja S., Nair A. B., Attimarad M., Venugopala K. N., *Nanomaterials*, **2021**, *11*, 1841
[191] Seo H. B., Gu M. B., *J. Bio. Eng.*, **2017**, *11*, 1
[192] Tabrizi M. A., Shamsipur M., Saber R., Sarkar S., *Anal. Chim. Acta*, **2017**, *985*, 61
[193] Zhou Y. L., Zhang H. Q., Liu L. T., Li C. M., Chang Z., Zhu X., Ye B. X., Xu M. T., *Sci. Rep.*, **2016**, *6*, 35186
[194] Hwang J., Seo Y., Jo Y., Son J., Choi J., *Sci. Rep.*, **2016**, *6*, 34778
[195] Walia S., Chandrasekaran A. R., Chakraborty B., Bhatia D., *ACS Appl. Bio Mater.*, **2021**, *4*, 5392
[196] Hartshorn C. M., Bradbury M. S., Lanza G. M., Nel A. E., Rao J., Wang A. Z., Wiesner U. B., Yang L., Grodzinski P., *ACS Nano*, **2018**, *12*, 24
[197] Manochehry S., McConnell E. M., Li Y., *Sci. Rep.*, **2019**, *9*, 1
[198] Boyacioglu O., Stuart C. H., Kulik G., Gmeiner W. H., *Mol. Ther. Nucleic Acids*, **2013**, *2*, e107
[199] Mairal T., Nadal P., Svobodova M., O'Sullivan C. K., *Biosens. Bioelectron.*, **2014**, *54*, 207
[200] Zhang Z., Pandey R., Li J., Gu J., White D., Stacey H. D., Ang J. C., Steinberg C. J., Capretta A., Filipe C. D. M., Mossman K., Balion C., Miller M. S., Salena B. J., Yamamura D., Soleymani L., Brennan J. D., Li Y., *Angew. Chem. Int. Ed.*, **2021**, *60*, 24266
[201] Vasudevan M., Tai M. J. Y., Perumal V., Gopinath S. C. B., Murthe S. S., Ovinis M., Mohamed N. M., Joshi N., *Biotechnol. Appl. Biochem.*, **2021**, *68*, 1386
[202] Zeng R. J., Su L. S., Luo Z. B., Zhang L. J., Lu M. H., Tang D. P., *Anal. Chim. Acta*, **2018**, *1038*, 21
[203] Kim G., Kim J., Kim S. M., Kato T., Yoon J., Noh S., Park E. Y., Park C., Lee T., Choi J. W., *Sens. Actuators B Chem.*, **2022**, *352*, 131060
[204] Wang Q. P., Zheng H. Y., Gao X. Y., Lin Z. Y., Chen G. N., *Chem. Commun.*, **2013**, *49*, 11418
[205] Yang X., Lv J. J., Yang Z. H., Yuan R., Chai Y. Q., *Anal. Chem.*, **2017**, *89*, 11636
[206] Yu H. Y., Zhao Z., Xiao B. C., Deng M. H., Wang Z. L., Li Z. Q., Zhang H. B., Zhang L., Qian J. W., Li J. H., *Anal. Chem.*, **2021**, *93*, 13673
[207] Schoukroun Barnes L. R., Wagan S., White R. J., *Anal. Chem.*, **2014**, *86*, 1131